European Journal of Medicinal Chemistry 74 (2014) 703–716

Contents lists available at ScienceDirect

European Journal of Medicinal Chemistry

journal homepage: http://www.elsevier.com/locate/ejmech

Original article

Benzothiazole head group based cationic lipids: Synthesis and application for gene delivery

Bhavani Kedika, Srilakshmi V. Patri*

Department of Chemistry, National Institute of Technology, Warangal 506004, Andhra Pradesh, India

ARTICLE INFO

Article history:
Received 15 January 2013
Received in revised form
27 August 2013
Accepted 28 August 2013
Available online 21 September 2013

Keywords:
Gene delivery
Cationic liposome
Lipoplexes
Reducible tocopherol-based cationic amphiphiles
Lipofection
DNA release

ABSTRACT

A series of benzothiazole based lipids (**1**–**10**) containing different derivatives of benzothiazole in the head group region were synthesized to determine the structure–activity relationship for gene delivery. The liposomes formulated were mixed with plasmid DNA encoding green fluorescent protein (α5GFP) or β-galactosidase (*p*CMV-SPORT-β-gal) and transfected into B16F10 (Human melanoma cancer cells), CHO (Chinese hamster ovary), A-549 (Human lung carcinoma cells) and MCF-7 (Human breast carcinoma cells) types of cell lines. The efficiencies of lipids **9** and **10** in particular, were found to be comparable and even more when compared to that of LipofectAmine-2000. The transfection profiles of the efficient lipids are proved to be maintained even in the presence of serum. Thus, the benzothiazole head group based lipids developed have the potential to be used as transfection reagents in vitro and in vivo.

1. Introduction

The Field of cationic lipids, pioneered by Felgner [1,2], Behr [3,4], and Huang [5,6], has evolved exponentially, so that many different compounds have been reported [4,7–10]. They include diverse kinds of cationic lipids such as glycerol backbone [11], cholesterol based [6], aliphatic-hydrocarbon-tail based [12] and tocopherol based lipids [13,14]. Despite tremendous progresses, the therapeutic efficiency of cationic lipid-based transfection systems remains relatively low as compared to viral ones. This is largely due to incompatibilities between the lipid structure in the lipoplexes and the structure of the various physiological barriers encountered in vivo by the plasmid in the lipoplex on its way to the nucleus of target cells [15,16]. These incompatibilities can result in inefficient delivery of the required gene and in cytotoxic effects. Some of these problems are associated with the cationic nature of the vectors [17]. A solution found to circumvent these problems is to spread the positive charge of the cationic head by delocalizing it into a heterocyclic ring.

Upon the invention of pyridinium-based cationic lipids in 1940s, various heterocyclic cationic lipids had been studied and used for gene delivery. They include a series of these pyridinium heterocyclic ring based lipids [18,19], lipids with imidazolium polar heads [20], glycerol- and cholesterol-based positively charged heterocyclic amphiphiles [21,22] and Gemini lipids with aromatic backbone [23]. Heterocyclic cationic lipids containing imidazolium or pyridinium polar heads [19,20] have been reported to display higher transfection efficiencies and reduced cytotoxicity when compared with classical transfection systems.

In our continuous upsurge of designing novel and efficient vectors in the field of cationic lipid gene delivery, we exploited the positive charge delocalizing property of benzothiazole moiety in designing new series of lipids. Benzothiazole template is a privileged structure fragments in modern medicinal chemistry considering its broad pharmacological spectrum and affinity for various biotargets of these class heterocyclic compounds. Aminobenzothiazoles and related heterocycles represent a novel class of potent and selective antitumor agents which exhibit nanomolar inhibitory activity against a range of human breast, lung, colon, leukemia, CNS, melanoma, ovarian, renal and prostate cell lines

Abbrevations: Lipofect, LipofectAmine-2000; DMEM, Dulbecco's modified Eagle's medium; DMAP, 4-(dimethylamino)pyridine; FBS, fetal bovine serum; PBS, phosphate-buffered saline; ONPG, *O*-nitrophenyl-β-D-galactopyranoside.

* Corresponding author. Tel.: +91 870 2462672; fax: +91 870 2459547.
E-mail addresses: pv_slakshmi@yahoo.com, patrisrilakshmi@gmail.com, patrisrilakshmi@nitw.ac.in (S.V. Patri).

0223-5234/$ – see front matter © 2013 Elsevier Masson SAS. All rights reserved.
http://dx.doi.org/10.1016/j.ejmech.2013.08.034

in vitro [24,25]. Benzothiazoles are used as organic NIR (Near-infrared) fluorophores and have been found to be the most useful [26]. Their physical properties, biodistribution, pharmacokinetics and applications for in vivo fluorescence imaging have been summarized [27,28].

To the best of our knowledge, there is no example using benzothiazole as the hydrophilic head group of cationic lipid for gene delivery. In the present study, we designed and synthesized a series of cationic lipids (**1**–**10**) with benzothiazole derivatives in the head group region of lipids. Their interactions with plasmid DNA and the properties of formed lipoplexes were examined. The in vitro transfection efficiencies towards four cell lines were investigated to study the SAR (structure activity relationship) of this type of cationic lipids in gene delivery. Results indicated that small changes in the lipid structure such as replacement of a nitro group with an amino group or methoxy group with a hydroxyl group or changes in the chain length attached (C_{16} and C_{18}) might lead to essential distinction in the in vitro transfection efficiencies. Lipids **9** and **10** with amine group as substituent have much higher reporter gene transfection efficiency than LipofectAmine-2000 in CHO and MCF-7 types of cells.

2. Results and discussion

The present work illustrates the synthesis of lipids **1**–**10** with benzothiazole derivatives in the head group region and their physicochemical characteristics. The results of in vitro transfection experiments performed on four different types of cell lines to assess the transfection efficiencies of lipids **1**–**10** are reported. In addition, the inverted fluorescent microscope experiments in support of the results obtained in in vitro transfection studies are reported. A study of cytotoxicity in all the four types of cell lines used for transfection experiments and serum compatibility of transfection efficient lipids (**5**, **6**, **9** and **10**) in four types of cell lines are also reported.

2.1. Chemistry

The synthesized lipids **1**–**10** (Chart 1) described herein show some common structural features which include (a) presence of derivatives of benzothiazoles in the head group region and (b) the presence of *n*-hexadecyl or *n*-octadecyl group in the hydrophobic region. The details of the synthetic procedures for all the novel transfection lipids shown in Chart 1 are described in the Experimental section. As outlined in Scheme 1 (A, B, C), the reactions involved in preparing these new lipids are straightforward. Cationic lipids **1**–**4**, **7** and **8** were synthesized by the *N*-alkylation reaction with derivatives of 2-amino benzothiazoles available commercially to yield the respective intermediate tertiary amines. The resulting tertiary amine intermediates upon quaternization with excess methyliodide followed by chloride ion exchange over Amberlyst-26 yielded lipids **1**–**4**, **7** and **8** (Scheme 1 (A, B, C)). Lipids **5** and **6** were synthesized from lipids **3** and **4** respectively by demethylation of methoxy group present on these lipids. Similarly, lipids **9** and **10** were yielded respectively by reduction of nitro group present on lipids **7** and **8**. Structures of all the synthetic intermediates and final lipids shown in Scheme 1 (A, B, C) are confirmed by ^{1}H NMR and molecular ion peaks in their ESI mass spectra.

2.2. Liposomal formation

Liposomes could be conveniently prepared from a mixture of lipid with varying amounts of cholesterol, 1,2-dioleoyl-*sn*-glycero-phosphoethanolamine (DOPE) and 1,2-dioleoyl-*sn*-glycero-3-phosphocholine (DOPC) as colipids. Out of various combinations of mole ratios of lipid to colipid (0.5:0.5, 1:1, 1:2, 1:3, and 1:4) tried, it is found that a 1:1 molar ratio of lipid and colipid is found to form optically transparent suspensions. For the present lipids **1**–**10**, cholesterol was found to be a more efficacious colipid when compared to DOPC and DOPE (data not shown). This may be due to the greater steric requirements of the benzothiazole polar head, which favor cholesterol over DOPE and DOPC as reported earlier [17]. The beneficial effect of cholesterol for the fluidity of bilayers made out of lipids with an elevated critical temperature is well documented [29]. Liposomes were prepared under sterile conditions and were sonicated for 5 min at room temperature before transfection experiments. The vesicular suspensions were found to be stable even after two months if stored at 4 °C (stability studies, Supporting information).

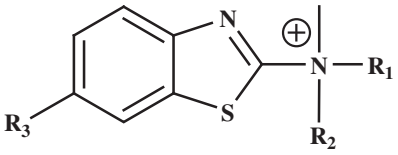

Lipid 1: R_1,R_2 = $C_{16}H_{33}$; R_3=H

Lipid 2: R_1,R_2 = $C_{18}H_{37}$; R_3=H

Lipid 3: R_1,R_2 = $C_{16}H_{33}$; R_3=OCH_3

Lipid 4: R_1,R_2 = $C_{18}H_{37}$; R_3=OCH_3

Lipid 5: R_1,R_2 = $C_{16}H_{33}$; R_3=OH

Lipid 6: R_1,R_2 = $C_{18}H_{37}$; R_3=OH

Lipid 7: R_1,R_2 = $C_{16}H_{33}$;R_3=NO_2

Lipid 8: R_1,R_2= $C_{18}H_{37}$; R_3=NO_2

Lipid 9: R_1,R_2 = $C_{16}H_{33}$; R_3=NH_2

Lipid 10: R_1,R_2 = $C_{18}H_{37}$; R_3=NH_2

Chart 1. Structure of lipids **1**–**10**.

2.3. Transfection biology

2.3.1. In vitro transfection studies

The relative in vitro gene delivery efficacies of lipids **1**–**10** in CHO, B16F10, A-549 and MCF-7 cells across the lipid:DNA charge ratios of 8:1 to 1:1 using cholesterol as colipid are summarized in Figs. 1–4. *p*CMV-SPORT-β-gal plasmid DNA was used as the reporter gene. The transfection efficiencies of the lipids **1**–**10** were compared with that of the LipofectAmine-2000. The results of Figs. 1–4 summarize the following transfection profiles. The transfection results reveal that there exists a difference in transfection profiles of benzothiazole based lipids **1**–**10** based on hydrophobic group. When comparing similar pairs across all experiments, it is found that among the pairs 1/2, 3/4, and 9/10, lipids with C_{16} performs better than lipids with C_{18} nearly 70% of time, and among the pairs 5/6 and 7/8, lipids with C_{16} and C_{18} perform nearly 50% of time better than each other.

Among lipids **1**–**10**, lipids **5**, **6** with hydroxyl group and lipids **9**, **10** with amino group substituents respectively at the 6-position of

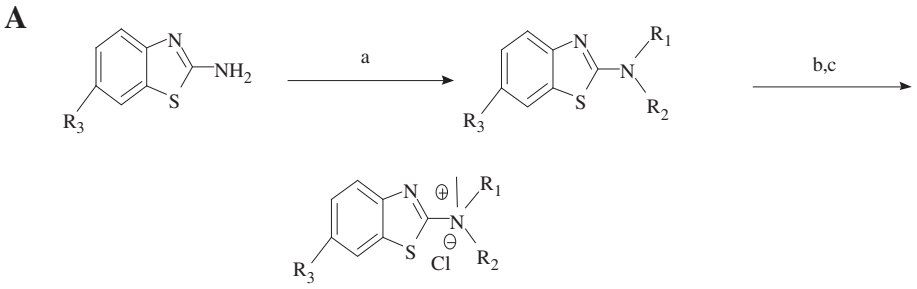

Lipid **1**: $R_1,R_2 = C_{16}H_{33}$; R_3=H

Lipid **2**: $R_1,R_2 = C_{18}H_{37}$; R_3=H

Lipid **3**: $R_1,R_2 = C_{16}H_{33}$; R_3=OCH_3

Lipid **4**: $R_1,R_2 = C_{18}H_{37}$; R_3=OCH_3

Lipid **7**: $R_1,R_2 = C_{16}H_{33}$;R_3=NO_2

Lipid **8**: R_1,R_2= $C_{18}H_{37}$; R_3=NO_2

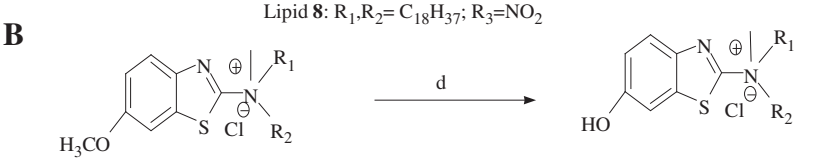

Lipid **3**: $R_1,R_2 = C_{16}H_{33}$; R_3=OCH_3

Lipid **4**: $R_1,R_2 = C_{18}H_{37}$; R_3=OCH_3

Lipid **5**: $R_1,R_2 = C_{16}H_{33}$; R_3=OH

Lipid **6**: $R_1,R_2 = C_{18}H_{37}$; R_3=OH

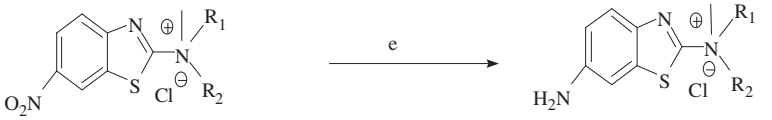

Lipid **7**: $R_1,R_2 = C_{16}H_{33}$;R_3=NO_2

Lipid **8**: R_1,R_2= $C_{18}H_{37}$; R_3=NO_2

Lipid **9**: $R_1,R_2 = C_{16}H_{33}$;R_3=NH_2

Lipid **10**: R_1,R_2= $C_{18}H_{37}$; R_3=NH_2

[a]Reagents: a) n-hexadecyl bromide/n-octadecyl bromide, K_2CO_3, dry DMF, rt, 24 h b) MeI, K_2CO_3,rt,48 h c) Amberlyst anion exchange resin, d) Pyridine hydrochloride,, reflux, 4 h , e) Zn-CH_3COOH, reflux, 3 h

Scheme 1. Synthesis of lipids **1**–**10**.[a]

benzothiazole head group were found to be transfection efficient. Whereas, lipids **1**, **2** with no substituent, lipids **3**, **4** with methoxy group and lipids **7**, **8** with nitro group substituents respectively at the 6-position of the benzothiazole head group were found to be inefficient in transfecting all the four types of cell lines used for in vitro transfection studies. The highest transfection efficiencies of all the transfection efficient lipids **5**, **6**, **9** and **10** were found to be at lipid:DNA charge ratios of 8:1. In general, lipids **9** and **10** with amino substituent were found to be the more transfection efficient among the present series of lipids in all the four types of cell lines studied and across majority of the lipid:DNA charge ratios. In particular lipid **9** with *n*-hexadecyl hydrophobic group and amino substituent at the 6-position of benzothiazole head group was found to be the highest transfection efficient lipid among lipids **1**–**10** studied. It is also observed from the results that, the transfection efficiency of lipid **9** at lipid:DNA charge ratio of 8:1 is found to be nearly four times higher in CHO and two times higher in MCF-7 type of cells compared to LipofectAmine-2000. In B16F10 and A549 types of cells the transfection efficiency of lipid **9** is found to be comparable with that of LipofectAmine-2000. The control experiments were carried out with cells containing DNA alone and cell alone (using the same amount of DNA as for lipids). The values taken for plotting the graphs are the original absorbance minus the absorbance from controls (whichever is highest) and thus ruling

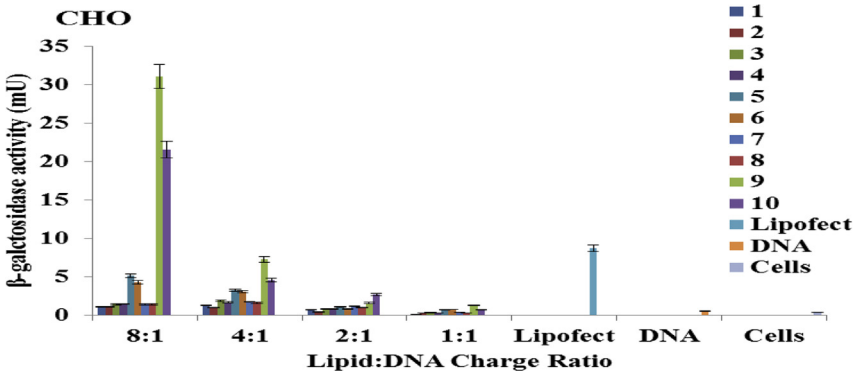

Fig. 1. In vitro gene delivery efficiencies of lipids **1**–**10** in CHO cells. Units of β-galactosidase activity were plotted against the varying lipid:DNA charge ratios (8:1–1:1). The transfection efficiencies of the lipids were compared to that of LipofectAmine-2000. The average control data of DNA alone and cells alone are also shown. Transfection experiments were performed as described in the text. All the lipids were tested on the same day, and the data presented are the average of three experiments performed on three different days. The error bar represents the standard error. The difference in the data obtained is statistically significant in all charge ratios (P <0.005).

out the possibility of cells or DNA interfering in the transfection results. The average control data of DNA alone and cells alone were shown in Figs. 1–4.

In the reporter gene assay, the in vitro gene transfer efficiencies of lipids **1**–**10** in general are found to be higher in CHO cells when compared to other three types of cancer cells i.e. MCF-7, B16F10, A-549. In the present study the very low transfection profiles of lipids **1**–**10** are observed in A-549 cells. The contrasting transfection profiles of lipids **5**, **6** compared to lipids **3**, **4** and similarly of lipids **9**, **10** compared to lipids **7**, **8** are expected because of the favorable hydrogen bonding interactions due to the presence of hydroxyl and amine groups in the head group region of lipids **5**, **6** and **9**, **10** respectively as reported earlier. It is also found that lipids **9** and **10** with amine group in the head group region are better transfection efficient than lipids **5** and **6** with hydroxyl group in the head group region. These observations are consistent with the previously demonstrated superior gene transfer properties of glycerol as well as non-glycerol based cationic lipids with amine head group functionalities to their hydroxy counterparts [30,31]. Taken together, the transfection profiles for the presently described benzothiazole head group based cationic amphiphiles summarized in Figs. 1–4 convincingly demonstrate that covalent grafting of amino and hydroxyl group functionalities in the head group region impart higher transfection properties to benzothiazole based cationic lipids. The presence of amine group shows greater increase in transfection profiles compared to hydroxyl groups for the presently studied series of lipids.

2.3.2. Transfection biology in presence of serum

The gene transfer efficacies of cationic amphiphiles in presence of serum are very important in order to use these lipids in in vivo studies [32,33]. Generally, serum-incompatibility of cationic transfection lipids is believed to begin via adsorption of negatively charged serum proteins onto the positively charged cationic liposome surfaces preventing their efficient interaction with cell surface and/or internalization [34,35]. Hence, the in vitro gene transfer efficacies of cationic amphiphiles usually get adversely affected in the presence of serum [36,37]. Towards probing the serum compatibility of the transfection efficient lipids (**5**, **6**, **9** and **10**), the transfection efficiencies of these lipids in all the four types of cells used for transfection at lipid:DNA charge ratio 8:1 (at which these lipids showed their higher transfection ability) in presence of increasing amounts of added serum (0–50%, v/v) were evaluated. The in vitro gene transfer efficacies of lipids **5**, **6**, **9** and **10** were in general found to be unaffected in the presence of serum of up to 10% of added serum as demonstrated through Fig. 5. The lipid **9** was found to be the highest serum compatible throughout the serum concentrations. Lipid **10** is also found to be serum compatible in all the other three types of cells except in CHO cells. The serum compatible transfection characteristics of the lipids studied (**5**, **6**, **9**

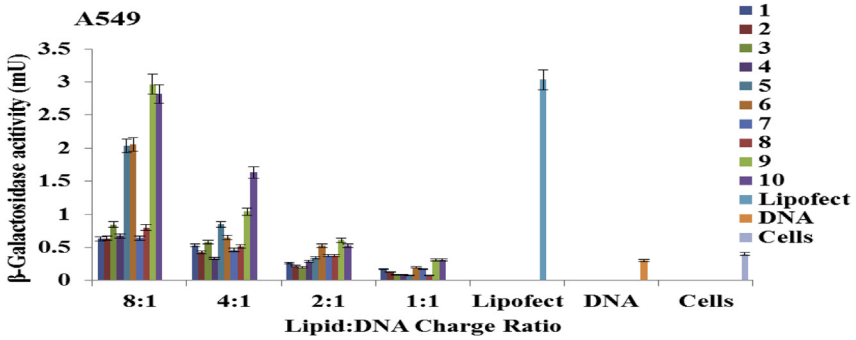

Fig. 2. In vitro gene delivery efficiencies of lipids **1**–**10** in A549 cells. Units of β-galactosidase activity were plotted against the varying lipid:DNA charge ratios (8:1–1:1). The transfection efficiencies of the lipids were compared to that of LipofectAmine-2000. The average control data of DNA alone and cells alone are also shown. Transfection experiments were performed as described in the text. All the lipids were tested on the same day, and the data presented are the average of three experiments performed on three different days. The error bar represents the standard error. The difference in the data obtained is statistically significant in all charge ratios (P <0.005).

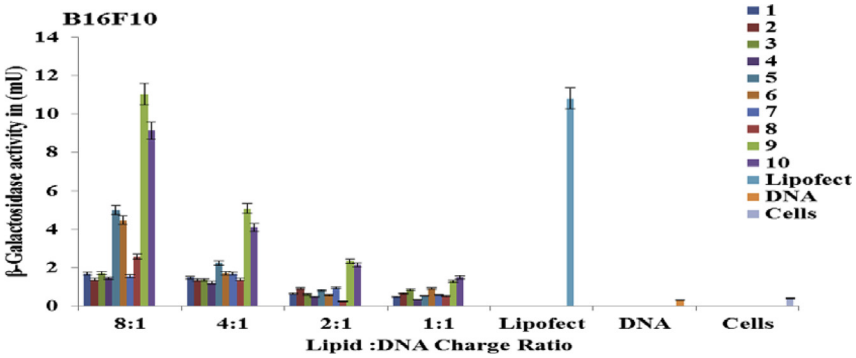

Fig. 3. In vitro gene delivery efficiencies of lipids **1**–**10** in B16F10 cells. Units of β-galactosidase activity were plotted against the varying lipid:DNA charge ratios (8:1–1:1). The transfection efficiencies of the lipids were compared to that of LipofectAmine-2000. The average control data of DNA alone and cells alone are also shown. Transfection experiments were performed as described in the text. All the lipids were tested on the same day, and the data presented are the average of three experiments performed on three different days. The error bar represents the standard error. The difference in the data obtained is statistically significant in all charge ratios (P <0.005).

and **10**) may be exploited in future for systemic in vivo gene transfection experiments and in designing of serum compatible benzothiazole based lipids.

2.4. α5GFP plasmid transfection

The relative transfection efficacies of lipids **1**–**10** were also evaluated by the in vitro transfection studies using α5GFP (a plasmid DNA encoding green fluorescence protein) in representative CHO (Fig. 6) cells using lipoplexes with 8:1 lipid:DNA charge ratio (the charge ratio where the lipids **1**–**10** showed higher transfection in CHO cells). After washing the cells with phosphate buffer saline, live CHO cells were viewed under an inverted fluorescence microscope. These microscopic cellular expressions demonstrate that lipoplexes of transfection efficient lipids showed better expression when compared to lipoplexes of transfection incompetent lipids (Fig. 6). Maximum expression of GFP in CHO cells was obtained with lipoplexes of lipid **9** and **10** at the given lipid:DNA charge ratio (Fig. 6), which is consistent with the results obtained from the in vitro transfection experiments. The very low GFP expression with lipoplexes of transfection inefficient lipids may be attributed to their inability in binding DNA at this given charge ratio.

2.5. Cellular uptake observed under inverted microscope

From the transfection results it is clear that among the lipids **1**–**10**, lipids **5**, **6**, and **9**, **10** showed their maximum transfection efficiencies at lipid:DNA charge ratio of 8:1. In order to verify whether the maximum uptake occurs for these lipids at this given charge ratio, A-549 cell lines were treated with lipoplexes comprising of *p*CMV-SPORT-β-gal plasmid DNA and rhodamine-PE labeled liposome of lipids **1**–**10** at the lipid:DNA charge ratio of 8:1. The cellular uptake of rhodamine-PE labeled liposomes was observed under inverted fluorescent microscope (Fig. 7). The findings demonstrate that maximum uptake is seen in the cells transfected with lipoplexes of lipids possessing hydroxyl and amino functionalities in their head group region (lipids **5**, **6**, **9** and **10**). The transfection inefficient lipids in which the amino and hydroxyl groups are replaced with nitro and methoxy groups respectively, in the head group region (lipids **3**, **4**, **7** and **8**) showed very little fluorescence at this given lipid:DNA charge ratio. Lipids **1** and **2** with no substituent in the head group region also showed very less uptake when compared to lipids **5**, **6**, **9** and **10**. The reason for the very low uptake of lipids **1** and **2** remains unclear at this point of investigation. Thus, these findings in the cellular uptake experiments (Fig. 7) support the notion that the varying transfection profiles of lipids **1**–**10** could be attributed to the cellular uptake variations of the respective lipids. This accentuates the supposition that the degree of cellular uptake plays an important role in modulating the transfection efficiencies of the presently described benzothiazole head group based cationic lipids.

2.6. Toxicity studies

MTT-based cell viabilities of lipids **1**–**10** were evaluated in all the four types of cells used for in vitro transfection (CHO, B16F10, A-549 and MCF-7) across the entire range of lipid:DNA charge ratios used

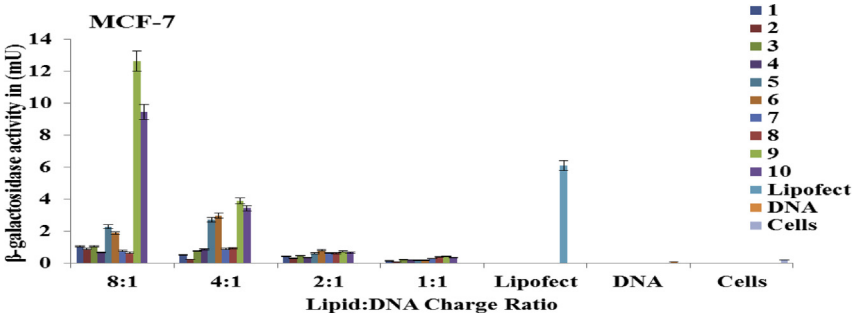

Fig. 4. In vitro gene delivery efficiencies of lipids **1**–**10** in MCF-7 cells. Units of β-galactosidase activity were plotted against the varying lipid:DNA charge ratios (8:1–1:1). The transfection efficiencies of the lipids were compared to that of LipofectAmine-2000. The average control data of DNA alone and cells alone are also shown. Transfection experiments were performed as described in the text. All the lipids were tested on the same day, and the data presented are the average of three experiments performed on three different days. The error bar represents the standard error. The difference in the data obtained is statistically significant in all charge ratios (P <0.005).

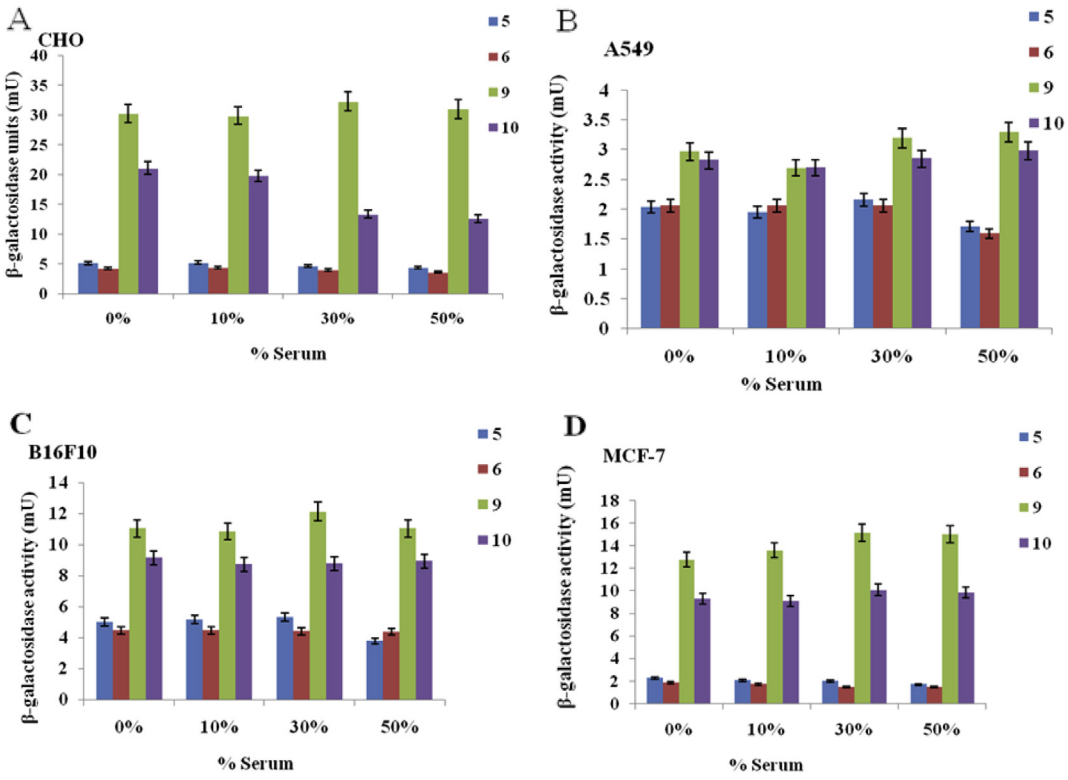

Fig. 5. Transfection efficacies of the cationic lipids **5**, **6**, **9** and **10** in the presence of increasing concentrations of added serum. In vitro transfection efficiencies of lipid:DNA complexes prepared using *p*CMV-β-gal-SPORT reporter gene at lipid:DNA charge ratio of 8:1 were evaluated in the presence of increasing concentrations of added serum in CHO (A), A-549 (B), B16F10 (C) and MCF-7 (D) types of cells. The error bar represents the standard error. The difference in the data obtained is statistically significant in all charge ratios ($P < 0.005$).

in the actual transfection experiments. Cell viabilities of all the lipids **1**–**10** in all four types of cell lines are found to be remarkably high (more than 85%) particularly up to the lipid:DNA charge ratios of 4:1 (Fig. 8). The cell viabilities of all the lipids **1**–**10** are found to be greater than or equal to 70% even at higher charge ratio of 8:1 (Fig. 8). Thus, the contrasting in vitro gene transfer efficacies of lipids **5**, **6**, **9** and **10** and **1**–**4**, **7** and **8** (Figs. 1–4) are unlikely to originate from varying cell cytotoxicities of the lipids.

2.7. Physicochemical characterizations of liposomes and lipoplexes

2.7.1. Lipid:DNA binding interactions and lipoplex sensitivities to DNase I

In order to characterize the electrostatic binding interactions between the plasmid DNA and the present cationic liposomes as a function of the lipid:DNA charge ratios, we performed both the conventional electrophoretic gel retardation assay and DNase I sensitivity assays for lipids **1**–**10** across the lipid:DNA charge ratios 1:1 to 8:1. Electrophoretic gel pattern observed in simple gel retardation assay (Fig. 9) revealed some interesting features. It is found that the transfection efficient lipids (**5**, **6**, **9** and **10**) were capable of completely inhibiting the electrophoretic mobility of plasmid DNA from lipoplexes prepared at high lipid:DNA charge ratio of 8:1 (Fig. 9). Whereas, the transfection inefficient lipids showed some free DNA even at this higher lipid:DNA charge ratio of 8:1. At lower lipid:DNA charge ratios of 4:1 to 1:1 lesser amount of free DNA was found in case of transfection efficient lipids when compared to transfection inefficient lipids. Such gel patterns are consistent with the notion that lower lipid:DNA binding interactions could play some role in eradicating the in vitro gene transfer efficacies of transfection inefficient lipids **1**–**4**, **7** and **8**. However, the higher lipid:DNA charge ratio may also cause lower transfection efficacies due to poor release of the complex from the endosome. Thus, the optimal lipid:DNA binding interactions may effectively facilitate the release of plasmid DNA in the cytoplasm after entering into the cell cytoplasm. Here, in the present case the optimal lipid:DNA binding of the transfection efficient lipids **5**, **6**, **9** and **10** may be at charge ratio of 8:1.

Next, with a view to obtaining insights into the accessibilities of the lipoplex associated DNA to DNase I, DNase I sensitivity assays were carried out across the entire range of lipid:DNA charge ratios of 1:1 to 8:1. After the free DNA digestion by DNase I, the total DNA (both digested and inaccessible DNA) was separated from the lipid and DNase I (by extracting with organic solvent) and loaded onto a 1% agarose gel. Resulting electrophoretic gel patterns in such DNase I protection experiments for lipoplexes prepared from lipids **1**–**10** are shown in Fig. 10. Among the two DNA lanes that are shown in Fig. 10 (A–E) one DNA lane corresponds to the digested DNA by DNase and the second one corresponds to the pure plasmid DNA. It was found that at all lipid:DNA charge ratios, the band intensities of inaccessible and therefore undigested DNA associated with transfection incompetent lipoplexes prepared from lipids **1**–**4**, **7** and **8** were observed to be significantly less than those associated with lipoplexes of transfection efficient lipids **5**, **6**, **9** and **10** (Fig. 10). This shows that the lipoplexes prepared from transfection efficient lipids are optimally stable when compared to the lipoplexes prepared from transfection inefficient lipids.

2.7.2. Nanosizes and global surface charges of the lipoplexes

It is observed that the nanosizes of lipoplexes prepared from both the transfection efficient and the incompetent lipids similarly increased with increasing lipid:DNA charge ratios within the range

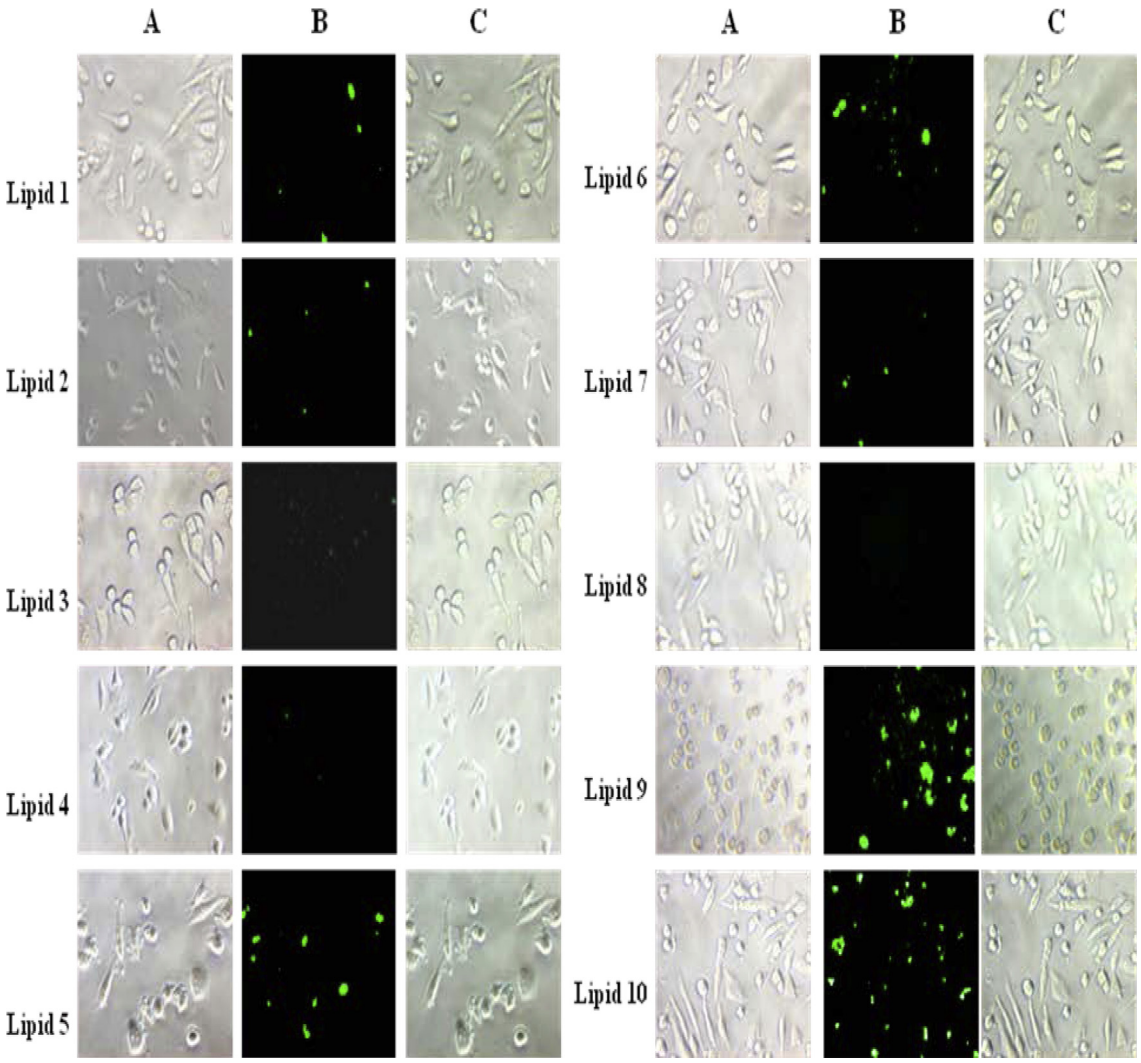

Fig. 6. Cellular expression of GFP. Inverted microscopic images of CHO cells transfected with lipoplexes of lipids **1**–**10** prepared at the highest in vitro transfection lipid:DNA charge ratios of 8:1 (A) Bright Field images, (B) fluorescent images and (C) overlay images. The details of the experiments are as described in the text.

of 300–890 nm. The surface potentials of lipid:DNA complexes was determined in presence of DMEM. It is observed that in majority of lipid:DNA complexes the positive charge is decreasing with increasing lipid:DNA charge ratios and moving towards negative charge also at higher lipid:DNA charge ratio. This may be attributed due to the negative components of the media which neutralizes the cationic charge on the lipid in the presence of DMEM. As the charge ratio increases, the rate of neutralization also increases and hence the charge on the lipoplexes decreases [38–41]. Taken together, the physicochemical characteristics summarized in Figs. 11 and 12 support the notion that both the surface potentials and nanosizes of lipoplexes are unlikely to play major roles in modulating the transfection efficacies of the present lipids.

3. Conclusions

In conclusion, we have demonstrated that a number of structural and formulation parameters including hydrophobic carbon chain lengths, lipid:colipid type, lipid:colipid ratios, lipid:DNA charge ratios and cell types play important roles in gene transfer and cytotoxicity of the benzothiazole based lipids studied. In vitro findings delineated that lipids **5**, **6** and lipids **9**, **10** with amino and hydroxyl substitutions respectively in the head group showed high gene transfer efficacies than lipids **1**–**4** with no substitution and lipids **3**, **4** and lipids **7**, **8** in which the hydroxyl and amino groups are replaced by methoxy and nitro groups respectively into multiple cultured mammalian cells including CHO, B16F10, MCF-7 and A549. Inverted fluorescence microscopic studies using lipoplexes containing green fluorescent protein encoding plasmid DNA demonstrated significantly higher expression of GFP with lipids **9** and **10** liposomes. The developed benzothiazole head group lipids are found to be serum compatible in all the four types of cell lines studied. The serum compatibility of the developed lipids combined with their NIR fluorophore properties can be exploited in the future in designing of efficient benzothiazole based cationic lipids for in vivo fluorescence imaging.

4. Experimental procedures

4.1. General procedures and materials

Mass spectral data were acquired by using a commercial LCQ ion trap mass spectrometer (ThermoFinnigan, SanJose, CA, USA) equipped with an ESI source. ^{1}H NMR spectra were recorded on a Varian FT 300 MHz NMR Spectrometer. Benzothiazol-2-amine, 6-methoxybenzothiazol-2-amine, 6-nitrobenzothiazol-2-amine

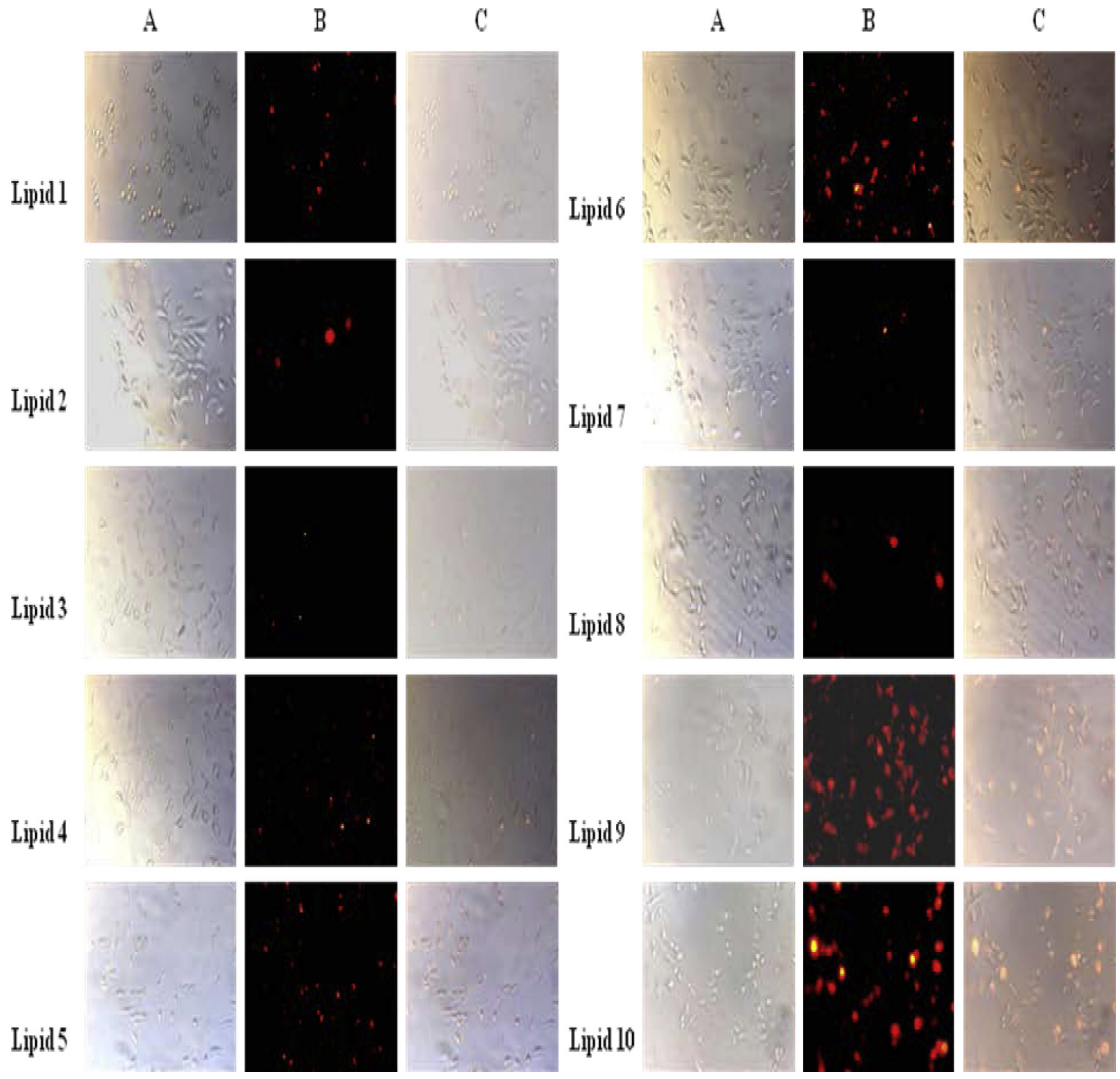

Fig. 7. Cellular uptake of rhodamine labeled lipoplexes. Inverted microscopic images of A-549 cells transfected with rhodamine labeled lipoplexes of lipids **1**–**10** prepared at the highest in vitro transfection lipid:DNA charge ratios of 8:1 (A) Bright Field images, (B) fluorescent images and (C) overlay images. The details of the experiments are as described in the text.

were purchased from Sigma Co. *p*CMV-SPORT-β-gal plasmid, α5GFP plasmid, rhodamine-PE and LipofectAmine-2000 were generous gift from IICT (Indian Institute of Chemical Technology), Hyderabad. Cell culture media, fetal bovine serum, 3-(4,5-dimethylthiazol-2-yl)-2,5-diphenyltetrazolium bromide (MTT), polyethylene glycol 8000, *o*-nitrophenyl-β-D-galactopyranoside were purchased from Sigma, St. Louis, USA. NP-40, antibiotics and agarose were purchased from Hi-media, India. Cholesterol, DOPE and DOPC was purchased from Fluka (Switzerland). Unless otherwise stated all the other reagents purchased from local commercial suppliers were of analytical grades and were used without further purification. The progress of the reaction was monitored by thin-layer chromatography using 0.25-mm silica gel plates. Column chromatography was performed with silica gel (Acme Synthetic Chemicals, India; finer than 200 & 60–120 mesh).

4.2. Synthesis

Synthetic routes for preparing cationic lipids **1**–**10** are shown schematically in parts A, B and C, Scheme 1, respectively. Details of the synthetic procedures, purifications and spectral characterizations of the lipids **1**–**10** as well as all their synthetic intermediates shown in Scheme 1 are described below.

4.2.1. Synthesis of lipid *1*: (Scheme 1, part A)

4.2.1.1. Synthesis of N,N-dihexadecyl benzothiazol-2-amine. To a solution of benzothiazol-2-amine (2.0 g, 13 mmol) in 10 mL of dry DMF, *n*-hexadecylbromide (8.9 g, 29 mmol), and catalytic amount of K_2CO_3 (0.18 g, 1.3 mmol) were added. The reaction mixture was stirred for 24 h at room temp. The reaction mixture was then poured into crushed ice in a beaker to obtain white solid which was filtered, washed with water and dried. The sample was purified by column chromatography using 60–120 mesh size silica gel and 1–2% of ethylacetate in hexane as eluent to afford the intermediate tertiary amine as a white solid (3.5 g, 44% yield, $R_f = 0.9$, 10% ethylacetate in hexane, m.p. 150–152 °C).

^{1}H NMR (300 MHz, $CDCl_3$) δ/ppm 0.81–0.95 [t, 6H, $J = 9$ Hz, (N–CH_2–CH_2–$(CH_2)_{13}$–C$\underline{H}_3$) × 2], 1.15–1.48 [m, 52H, (N–CH_2–CH_2–$(C\underline{H}_2)_{13}$–CH_3) × 2], 1.67–1.90 [m, 4H, (N–CH_2–C$\underline{H}_2$–$(CH_2)_{13}$–CH_3) × 2], 3.56–3.68 [t, 4H, J = 7.5 Hz, (N–C$\underline{H}_2$–CH_2–$(CH_2)_{13}$–

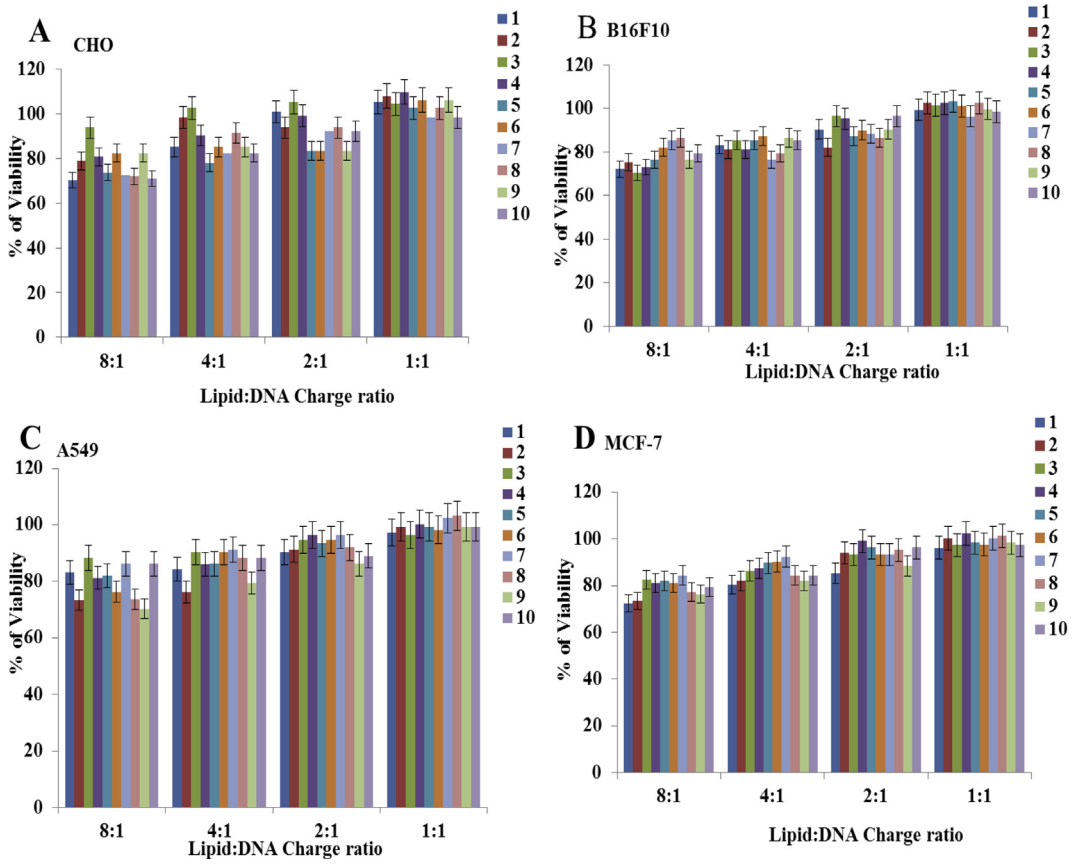

Fig. 8. Representative percent cell viabilities of lipids **1**–**10** in CHO, B16F10, A549 and MCF-7 types of cells using MTT assay. The absorption obtained with reduced formazan with cells in the absence of lipids was taken to be 100. The toxicity assays were performed as described in the text. The data presented are the average values of three independent experiments ($n = 3$).

CH_3) × 2], 7.23–7.41 [m, 2H, H-5, H-6-benzothiazole], 7.47–7.59 [m, 1H, H-7-benzothiazole], 7.72–7.84 [m, 1H, H-4-benzothiazole]. ESI-MS m/z: 600 $[M + H]^+$.

*4.2.1.2. Synthesis of N,N-dihexadecyl-N-methylbenzothiazol-2-ammonium chloride (lipid **1**, Scheme 1, part A).* In a 25 mL round bottomed flask, 2 mL of methyl iodide was added to intermediate tertiary amine (1.0 g, 1.6 mmol) prepared in step (a). The reaction mixture was stirred at room temperature for 12 h. The solvent from the reaction mixture was evaporated and dried. The residue upon column chromatographic purification using 60–120 mesh size silica gel, and 2% methanol in chloroform as eluent followed by chloride ion exchange (using Amberlyst A-26 with chloroform as eluent) afforded the pure title lipid **1** as a white solid (0.9 g, 88% yield, $R_f = 0.7$, 10% methanol in chloroform, m.p. 176–181 °C). ^{1}H NMR (300 MHz, $CDCl_3$) δ/ppm 0.81–0.91 [t, 6H, $J = 6$ Hz, (N–CH_2–CH_2–$(CH_2)_{13}$–$C\underline{H}_3$) × 2], 1.16–1.48 [m, 52H, (N–CH_2–CH_2–$(C\underline{H}_2)_{13}$–CH_3) × 2], 1.65–1.78 [m, 4H, (N–CH_2–$C\underline{H}_2$–$(CH_2)_{13}$–CH_3) × 2], 3.36 [s, 3H, N–$C\underline{H}_3$], 3.45–3.61 [m, 4H, (N–$C\underline{H}_2$–CH_2–$(CH_2)_{13}$–CH_3) × 2], 7.51–7.59 [m, 2H, H-5, H-6-benzothiazole], 7.75–7.82 [m, 2H, H-4, H-7-benzothiazole]. ESI-MS m/z: 615 $[M + H]^+$.

*4.2.2. Synthesis of N,N-dioctadecyl-N-methylbenzothiazol-2-ammonium chloride, lipid **2** (Scheme 1, part A)*

The title lipid **2** was synthesized following the same synthetic procedure as described for preparing lipid **1** using benzothiazol-2-amine and *n*-octadecylbromide. All the isolated intermediates gave spectroscopic data in agreement with their assigned structures shown in Scheme 1, part A.

^{1}H NMR (300 MHz, $CDCl_3$) of intermediate of lipid **2** (Scheme 1, part A, R_1, R_2 = *n*-octadecyl) δ/ppm 0.82–0.95 [t, 6H, $J = 4.5$ Hz, (N–CH_2–CH_2–$(CH_2)_{15}$–$C\underline{H}_3$) × 2], 1.15–1.41 [m, 60H, (N–CH_2–CH_2–$(C\underline{H}_2)_{15}$–CH_3) × 2], 1.61–1.79 [m, 4H, (N–CH_2–$C\underline{H}_2$–$(CH_2)_{15}$–CH_3) × 2], 3.58–3.68 [m, 4H, (N–$C\underline{H}_2$–CH_2–$(CH_2)_{15}$–CH_3) × 2], 7.29–7.41 [m, 2H, H-5, H-6-benzothiazole], 7.51–7.58 [m, 1H, H-7-benzothiazole], 7.74–7.85 [m, 1H, H-4-benzothiazole]. ESI-MS m/z: 655 $[M]^+$.

^{1}H NMR (300 MHz, $CDCl_3$) of lipid **2** (*N,N*-dioctadecyl-*N*-methylbenzothiazol-2-ammonium chloride) (Scheme 1, part A, R_1, R_2 = *n*-octadecyl) δ/ppm 0.79–0.90 [t, 6H, $J = 7.5$ Hz, (N–CH_2–CH_2–$(CH_2)_{15}$–$C\underline{H}_3$) × 2], 1.17–1.48 [m, 60H, (N–CH_2–CH_2–$(C\underline{H}_2)_{15}$–CH_3) × 2], 1.65–1.78 [m, 4H, (N–CH_2–$C\underline{H}_2$–$(CH_2)_{15}$–CH_3) × 2], 3.34–3.41 [s, 3H, N–$C\underline{H}_3$], 3.45–3.55 [m, 4H, (N–$C\underline{H}_2$–CH_2–$(CH_2)_{15}$–CH_3) × 2], 7.52–7.56 [m, 2H, H-5, H-6-benzothiazole], 7.71–7.76 [m, 2H, H-4, H-7-benzothiazole]. ESI-MS m/z: 670 $[M]^+$.

*4.2.3. Synthesis of lipid **3** (Scheme 1, part A)*

4.2.3.1. Synthesis of N,N-dihexadecyl-6-methoxybenzothiazol-2-amine. The tertiary amine intermediate was synthesized using 6-methoxybenzothiazol-2-amine (2.0 g, 11 mmol) as starting material and alkylated with *n*-hexadecylbromide (7.5 g, 24 mmol) following the same procedure as described in the preparation of lipid **1**. Silica gel column chromatographic purification using 1–2% ethylacetate in hexane afforded (3.8 g, 54% yield, $R_f = 0.9$, 10% ethylacetate in hexane, m.p. 168–174 °C) the intermediate tertiary amine as a white solid.

^{1}H NMR (300 MHz, $CDCl_3$) δ/ppm 0.85–0.95 [t, 6H, $J = 4.5$ Hz, (N–CH_2–CH_2–$(CH_2)_{13}$–$C\underline{H}_3$) × 2], 1.22–1.42 [m, 52H, (N–CH_2–CH_2–$(C\underline{H}_2)_{13}$–CH_3) × 2], 1.69–1.85 [m, 4H, (N–CH_2–$C\underline{H}_2$–$(CH_2)_{13}$–

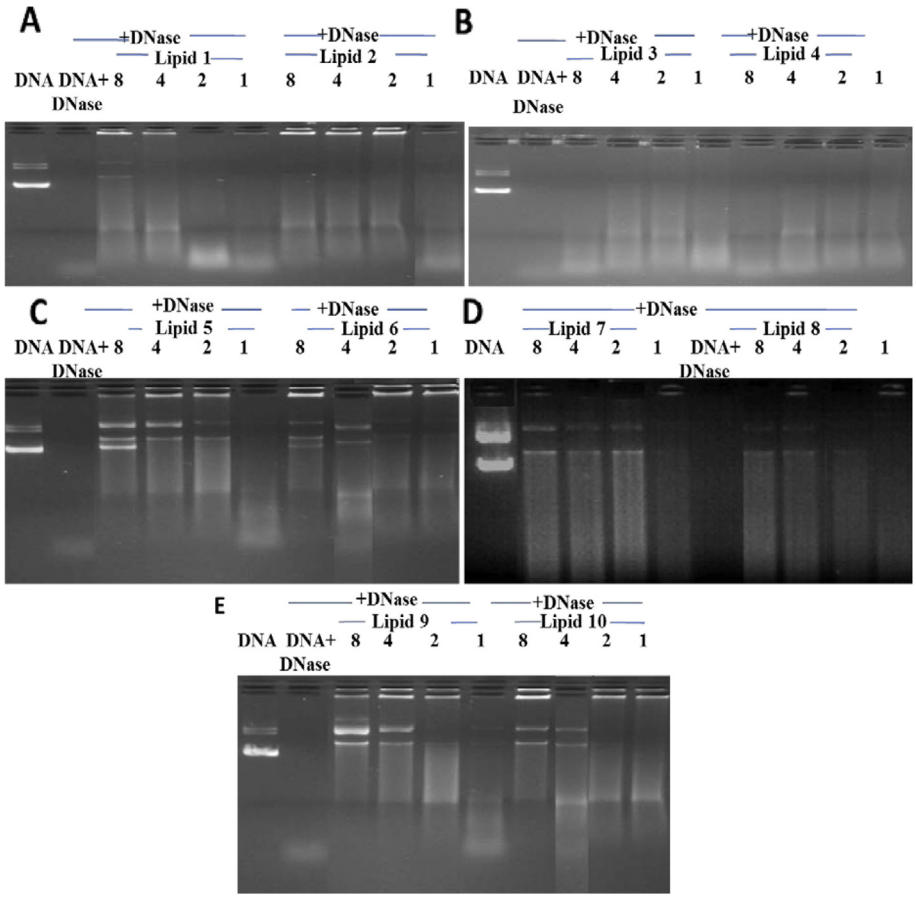

Fig. 9. Electrophoretic gel patterns for lipoplex-associated DNA in gel retardation assay. (A)–(E) Refer to lipids **1**–**10**. The lipid:DNA charge ratios are indicated at the top of each line. The details of the treatment are as described in the text.

CH_3) × 2], 3.32–3.48 [t, 4H, J = 6 Hz, (N–C$\underline{H}_2$–CH_2–$(CH_2)_{13}$–CH_3) × 2], 3.83 [s, 3H, OC$\underline{H}_3$–C_6H_5], 6.65–6.72 [m, 1H, H-5-benzothiazole], 6.82–6.85 [m, 1H, H-7-benzothiazole], 7.23–7.29 [m, 1H, H-4-benzothiazole]. ESI-MS m/z: 652 $[M + Na]^+$.

*4.2.3.2. Synthesis of N,N-dihexadecyl-6-methoxy-N-methyl-benzothiazol-2-ammonium chloride (lipid **3**, Scheme 1, part A).* The intermediate tertiary amine (1.0 g, 1.5 mmol) prepared above in step (a) was treated with 2 mL of methyl iodide following the same procedure as given in step (b) of synthesis of lipid **1** to yield (0.85 g, 83% yield, R_f = 0.8, 10% methanol in chloroform, m.p. 182–186 °C) lipid **3** as a white solid. ^{1}H NMR (300 MHz, $CDCl_3$) δ/ppm 0.85–0.91 [t, 6H, J = 6 Hz, (N–CH_2–CH_2–$(CH_2)_{13}$–C$\underline{H}_3$) × 2], 1.18–1.47 [m, 52H, (N–CH_2–CH_2–(C$\underline{H}_2$)$_{13}$–CH_3) × 2], 1.67–1.89 [m, 4H, (N–CH_2–C$\underline{H}_2$–$(CH_2)_{13}$–CH_3) × 2], 3.17 [s, 3H, N–C$\underline{H}_3$], 3.25–3.46 [m, 4H, (N–C$\underline{H}_2$–CH_2–$(CH_2)_{13}$–CH_3) × 2], 3.49 [s, 3H, OC$\underline{H}_3$–C_6H_5], 6.94–7.16 [m, 2H, H-5, H-7, –benzothiazole], 7.14–7.23 [m, 1H, H-4-benzothiazole]. ESI-MS m/z: 645 $[M + H]^+$.

*4.2.4. Synthesis of N,N-dioctadecyl-6-methoxy-N-methylbenzothiazol-2-ammonium chloride, lipid **4** (Scheme 1, part A)*

The title lipid **4** was synthesized following the same synthetic procedure as described for preparing lipid **3** using 6-methoxybenzothiazol-2-amine and *n*-octadecylbromide. All the isolated intermediates gave spectroscopic data in agreement with their assigned structures shown in Scheme 1, part A.

^{1}H NMR (300 MHz, $CDCl_3$) of intermediate of lipid **4** (Scheme 1, part A, R_3 = OCH_3, R_1, R_2 = *n*-octadecyl) δ/ppm 0.82–0.93 [t, 6H, J = 7.5 Hz, (N–CH_2–CH_2–$(CH_2)_{15}$–C$\underline{H}_3$) × 2], 1.12–1.48 [m, 60H, (N–CH_2–CH_2–(C$\underline{H}_2$)$_{15}$–CH_3) × 2], 1.61–1.78 [m, 4H, (N–CH_2–C$\underline{H}_2$–$(CH_2)_{15}$–CH_3) × 2], 3.41–3.58 [m, 4H, (N–C$\underline{H}_2$–CH_2–$(CH_2)_{15}$–CH_3) × 2], 3.90 [s, 3H, OC$\underline{H}_3$–C_6H_5], 6.36–6.48 [m, 1H, H-5, –benzothiazole], 6.62–6.67 [m, 1H, H-7-benzothiazole], 7.09–7.12 [m, 1H, H-4-benzothiazole]. ESI-MS m/z: 686 $[M + H]^+$.

^{1}H NMR (300 MHz, $CDCl_3$) of lipid **4** (*N,N*-dioctadecyl-6-methoxy-*N*-methylbenzothiazol-2-ammonium chloride) (Scheme 1, part A, R = OCH_3, R_1, R_2 = *n*-octadecyl) δ/ppm 0.78–0.85 [t, 6H, J = 4.5 Hz, (N–CH_2–CH_2–$(CH_2)_{15}$–C$\underline{H}_3$) × 2], 1.14–1.51 [m, 60H, (N–CH_2–CH_2–(C$\underline{H}_2$)$_{15}$–CH_3) × 2], 1.65–1.88 [m, 4H, (N–CH_2–C$\underline{H}_2$–$(CH_2)_{15}$–CH_3) × 2], 3.25 [s, 3H, N–C$\underline{H}_3$], 3.32–3.51 [m, 4H, (N–C$\underline{H}_2$–CH_2–$(CH_2)_{15}$–CH_3) × 2], 3.63 [s, 3H, OC$\underline{H}_3$–C_6H_5], 6.59–6.67 [m, 1H, H-5-benzothiazole], 6.78–6.91 [m, 1H, H-7-benzothiazole], 7.07–7.12 [m, 1H, H-4-benzothiazole]. ESI-MS m/z: 701 $[M + H]^+$.

*4.2.5. Synthesis of N,N-dihexadecyl-6-hydroxy-N-methylbenzothiazol-2-ammonium chloride, lipid **5** (Scheme 1, part B)*

The title lipid **5** was synthesized by demethylation of lipid **3**. In a 25 mL round bottom flask fitted with air condenser, 1.0 g of lipid **3** (1.5 mmol) and 0.7 g of pyridine hydrochloride (Py. HCl) (6 mmol) were taken and heated to a temperature of 180–190 °C. The reaction was performed as a melt. The reaction went smoothly to completion within 3 h. The reaction mixture was poured into ice cold water, extracted with ethylacetate (3 × 50 mL), organic layer was repeatedly washed with water, dried over sodium sulfate and evaporated under pressure to yield the crude product. The residue

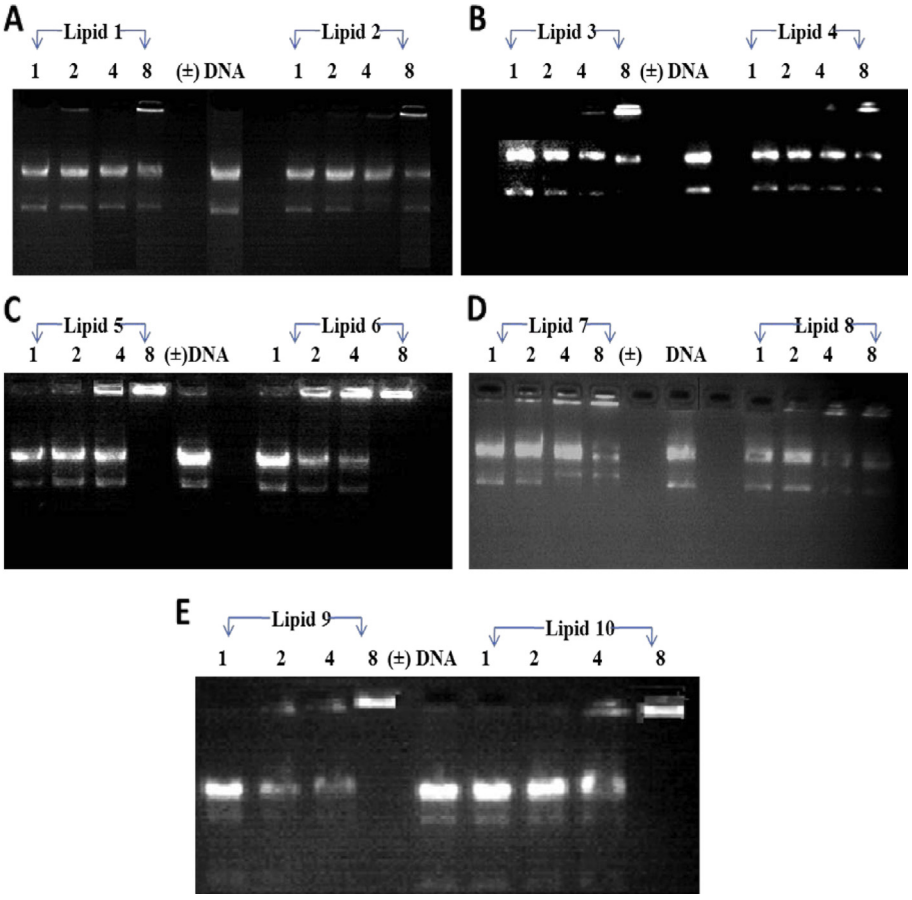

Fig. 10. Electrophoretic gel patterns for lipoplex-associated DNA in DNase I sensitivity assay. (A)–(E) Refers to lipids **1**–**10**. The lipid:DNA charge ratios are indicated at the top of each lane. The details of the treatment are as described in the text.

was purified by column chromatography using 60–120 mesh size silica gel and 2–3% of methanol in chloroform as eluent to afford iodide salt of lipid **5** (0.74 g, 76% yield, $R_f = 0.5$, 10% methanol in chloroform, m.p. 205–208 °C). Chloride ion exchange of iodide salt of lipid **5** (using Amberlyst A-26 with methanol as eluent) afforded the pure title lipid **5** as a white solid.

^{1}H NMR (300 MHz, DMSO) δ/ppm 0.75–0.85 [t, 6H, $J = 4.5$ Hz, (N–CH_2–CH_2–$(CH_2)_{13}$–CH_3) × 2], 1.21–1.42 [m, 52H, (N–CH_2–CH_2–$(CH_2)_{13}$–CH_3) × 2], 1.52–1.71 [m, 4H, (N–CH_2–CH_2–$(CH_2)_{13}$–CH_3) × 2], 3.88 [s, 3H, N–CH_3], 4.09–4.21 [t, 4H, $J = 5.4$ Hz, (N–CH_2–CH_2–$(CH_2)_{13}$–CH_3) × 2], 6.92 [d, 1H, $J = 6$ Hz, H-5, –benzothiazole], 7.34 [s, 1H, H-7, –benzothiazole], 7.49 [d, 1H, $J = 6$ Hz, H-4-benzothiazole], 9.78–9.95 [bs, 1H, –OH–C_6H_5]. ESI-MS m/z: 630 $[M]^+$.

4.2.6. Synthesis of N,N-dioctadecyl-6-hydroxy-N-methylbenzothiazol-2-ammonium chloride, lipid ***6*** *(Scheme 1, part B)*

The title lipid **6** was synthesized from lipid **4** following the same procedure as described in synthesis of lipid **5**.

^{1}H NMR (300 MHz, $CDCl_3$) δ/ppm 0.86–0.92 [t, 6H, $J = 7.5$ Hz, (N–CH_2–CH_2–$(CH_2)_{15}$–CH_3) × 2], 1.14–1.46 [m, 52H, (N–CH_2–CH_2–$(CH_2)_{15}$–CH_3) × 2], 1.61–1.72 [m, 4H, (N–CH_2–CH_2–$(CH_2)_{15}$–CH_3) × 2], 3.38 [s, 3H, N–CH_3], 3.58–3.71 [t, 4H, $J = 7.5$ Hz, (N–CH_2–CH_2–$(CH_2)_{15}$–CH_3) × 2], 6.71 [d, 1H, $J = 4.5$ Hz, H-5, –

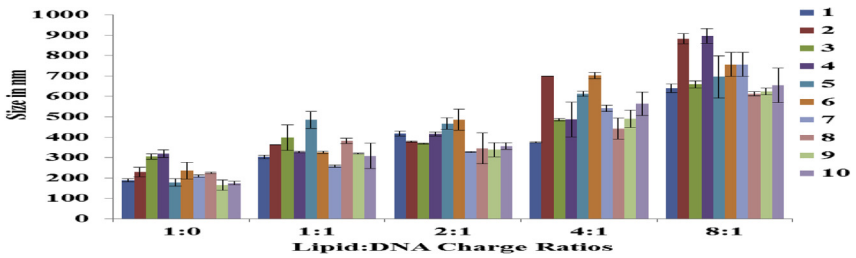

Fig. 11. Sizes (average hydrodynamic diameter) were measured by laser light scattering technique using Zetasizer nanoseries 500 (malvan Instruments, UK). Values shown are the averages obtained from three measurements. Individual sizes varied within 10-30% and the Polydispersity indices varied from 0.203 to 0.660. Lipoplex Sizes across the lipid:DNA charge ratios 1:1–8:1 measured in presence of DMEM.

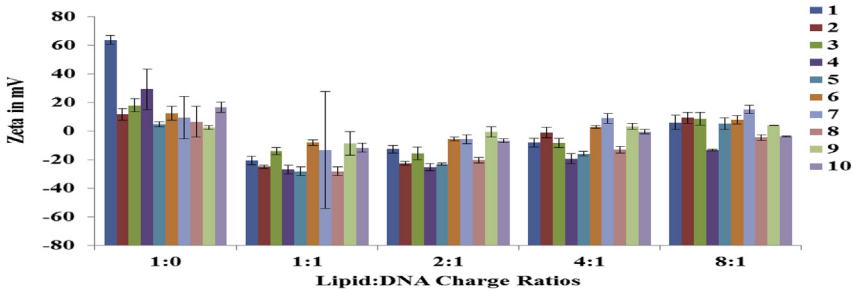

Fig. 12. Lipoplex zeta potentials (mV) across the lipid:DNA charge ratios 1:1–8:1 measured in presence of DMEM. Zeta potentials were measured by laser light scattering technique using Zetasizer 3000HA (Malvern Instruments, UK). Values shown are the averages obtained from ten measurements.

benzothiazole], 7.03 [s, 1H, H-7-benzothiazole], 7.25 [d, 1H, $J = 4.5$ Hz, H-4-benzothiazole], 9.31–9.37 [bs, 1H, –OH–C_6H_5]. ESI-MS m/z: 686 $[M]^+$.

4.2.7. Synthesis of lipid ***7*** *(Scheme 1, part A)*

4.2.7.1. Synthesis of N,N-dihexadecyl-6-nitrobenzothiazol-2-amine. The intermediate tertiary amine of lipid **7** was synthesized using 6-nitrobenzothiazol-2-amine (2.0 g, 10 mmol) and *n*-hexadecylbromide (6.9 g, 22 mmol) and following the same procedure as described for intermediate of lipid **1**. Silica gel column chromatographic purification using 2–3% ethylacetate in hexane afforded (5.1 g, 77% yield, R_f = 0.8, 10% ethylacetate in hexane, m.p. 224–227 °C) the intermediate tertiary amine as a pale yellow solid.

^{1}H NMR (300 MHz, $CDCl_3$) δ/ppm 0.81–0.92 [t, 6H, $J = 4.5$ Hz, (N–CH_2–CH_2–$(CH_2)_{13}$–CH_3) × 2], 1.18–1.45 [m, 52H, (N–CH_2–CH_2–$(CH_2)_{13}$–CH_3) × 2], 1.68–1.91 [m, 4H, (N–CH_2–CH_2–$(CH_2)_{13}$–CH_3) × 2], 3.42–3.55 [m, 4H, (N–CH_2–CH_2–$(CH_2)_{13}$–CH_3) × 2], 7.43 [d, 1H, $J = 6$ Hz, H-4, –benzothiazole], 8.15 [d, 1H, $J = 6$ Hz, H-5, –benzothiazole], 8.48 [s, 1H, H-7-benzothiazole]. ESI-MS m/z: 644 $[M]^+$.

4.2.7.2. Synthesis of N,N-dihexadecyl-N-methyl-6-nitrobenzothiazol-2-ammonium chloride (lipid ***7****, Scheme 1, part A).* *N*-Methylation of tertiary amine (1.0 g, 1.5 mmol) from the above step (a) was carried out following the same procedure as given in step (b) of synthesis of lipid **1** to yield (0.9 g, 90% yield, R_f = 0.6, 10% methanol in chloroform, m.p. 241–243 °C) pure lipid **7** as a yellow solid. ^{1}H NMR (300 MHz, $CDCl_3$) δ/ppm 0.91–0.95 [t, 6H, $J = 3$ Hz, (N–CH_2–CH_2–$(CH_2)_{13}$–CH_3) × 2], 1.16–1.45 [m, 52H, (N–CH_2–CH_2–$(CH_2)_{13}$–CH_3) × 2], 1.61–1.78 [m, 4H, (N–CH_2–CH_2–$(CH_2)_{13}$–CH_3) × 2], 3.32 [s, 3H, N–CH_3], 3.39–3.43 [m, 4H, (N–CH_2–CH_2–$(CH_2)_{13}$–CH_3) × 2], 7.55 [d, 1H, $J = 3$ Hz, H-5, –benzothiazole], 7.92–7.94 [d, 1H, $J = 3$ Hz, H-4, –benzothiazole], 8.15 [s, 1H, H-7-benzothiazole]. ESI-MS m/z: 660 $[M + H]^+$.

4.2.8. Synthesis of N,N-dioctadecyl-N-methyl-6-nitrobenzothiazol-2-ammonium chloride lipid ***8*** *(Scheme 1, part A)*

The title lipid **8** was synthesized following the same synthetic procedure as described in the preparation of lipid **7** using 6-nitrobenzothiazol-2-amine and *n*-octadecylbromide. All the isolated intermediates gave spectroscopic data in agreement with their assigned structures shown in Scheme 1, part A.

^{1}H NMR (300 MHz, $CDCl_3$) of intermediate of lipid **4** (Scheme 1, part A, R = NO_2, R_1, R_2 = *n*-octadecyl) δ/ppm 0.78–0.95 [t, 6H, $J = 4.5$ Hz, (N–CH_2–CH_2–$(CH_2)_{15}$–CH_3) × 2], 1.18–1.45 [m, 60H, (N–CH_2–CH_2–$(CH_2)_{15}$–CH_3) × 2], 1.69–1.85 [m, 4H, (N–CH_2–CH_2–$(CH_2)_{15}$–CH_3) × 2], 3.45–3.55 [t, 4H, $J = 9$ Hz, (N–CH_2–CH_2–$(CH_2)_{15}$–CH_3) × 2], 7.55 [d, 1H, $J = 6$ Hz, H-4-benzothiazole], 8.21 [d, 1H, $J = 6$ Hz, H-5, –benzothiazole], 8.49 [s, 1H, H-7-benzothiazole]. ESI-MS m/z: 700 $[M]^+$.

^{1}H NMR (300 MHz, $CDCl_3$) of lipid **8** (*N,N*-dioctadecyl-*N*-methyl-6-nitrobenzothiazol-2-ammonium chloride) (Scheme 1, part A, R = NO_2, R_1, R_2 = *n*-octadecyl) δ/ppm 0.78–0.96 [t, 6H, $J = 7.5$ Hz, (N–CH_2–CH_2–$(CH_2)_{15}$–CH_3) × 2], 1.15–1.46 [m, 60H, (N–CH_2–CH_2–$(CH_2)_{15}$–CH_3) × 2], 1.61–1.82 [m, 4H, (N–CH_2–CH_2–$(CH_2)_{15}$–CH_3) × 2], 3.31 [s, 3H, N–CH_3], 3.42–3.55 [t, 4H, $J = 6.6$ Hz, (N–CH_2–CH_2–$(CH_2)_{15}$–CH_3) × 2], 7.58 [d, 1H, $J = 3$ Hz, H-4, –benzothiazole], 8.18 [d, 1H, $J = 3$ Hz, H-5-benzothiazole], 8.47 [s, 1H, H-7-benzothiazole]. ESI-MS m/z: 715 $[M]^+$.

4.2.9. Synthesis of 6-amino-N-methyl-N,N-dihexadecylbenzothiazol-2-ammonium chloride, lipid ***9*** *(Scheme 1, part C)*

The title lipid **9** was synthesized by the reduction of nitro group in lipid **7**. The nitro compound, lipid **7** (1.0 g, 1.5 mmol) was dissolved in 6 mL of 1:1 mixture of glacial acetic acid and ethanol followed by the addition of 0.3 g of zinc dust. The mixture was stirred for 4 h at 60 °C under nitrogen atmosphere. After cooling, the mixture was filtered and the solvent was evaporated under vacuum from the filtrate. The residue was dissolved in ethylacetate and washed with dilute sodium hydroxide solution and dried over $MgSO_4$. Evaporation of the solvent affords the crude product. The residue was purified by column chromatography using 60–120 mesh size silica gel and 3–4% of methanol in chloroform as eluent to afford iodide salt of lipid **9** (0.7 g, 75% yield, R_f = 0.4, 10% methanol in chloroform, m.p. 254–258 °C). Chloride ion exchange of iodide salt of lipid **9** (using Amberlyst A-26 with methanol as eluent) afforded the pure title lipid **9** as light yellow solid.

^{1}H NMR (300 MHz, $CDCl_3$) δ/ppm 0.78–0.92 [t, 6H, $J = 7.5$ Hz, (N–CH_2–CH_2–$(CH_2)_{13}$–CH_3) × 2], 1.12–1.48 [m, 52H, (N–CH_2–CH_2–$(CH_2)_{13}$–CH_3) × 2], 1.65–1.78 [m, 4H, (N–CH_2–CH_2–$(CH_2)_{13}$–CH_3) × 2], 3.76 [s, 3H, N–CH_3], 3.82–3.91 [t, 4H, $J = 6$ Hz, (N–CH_2–CH_2–$(CH_2)_{13}$–CH_3) × 2], 4.22–4.45 [bs, 2H, –NH_2–C_6H_5], 6.64 [d, 1H, $J = 4.5$ Hz, H-5-benzothiazole], 6.87 [s, 1H, H-7-benzothiazole], 7.11 [d, 1H, $J = 4.5$ Hz, H-4-benzothiazole]. ESI-MS m/z: 630 $[M]^+$.

4.2.10. Synthesis of 6-amino-N-methyl-N,N-dioctadecylbenzothiazol-2-ammonium chloride, lipid ***10*** *(Scheme 1, part C)*

The title lipid **10** was synthesized from lipid **8** following the same procedure as described in synthesis of lipid **9**.

^{1}H NMR (300 MHz, $CDCl_3$) δ/ppm 0.76–0.91 [t, 6H, $J = 4.8$ Hz, (N–CH_2–CH_2–$(CH_2)_{15}$–CH_3) × 2], 1.12–1.43 [m, 60H, (N–CH_2–CH_2–$(CH_2)_{15}$–CH_3) × 2], 1.67–1.91 [m, 4H, (N–CH_2–CH_2–$(CH_2)_{15}$–CH_3) × 2], 3.35 [s, 3H, N–CH_3], 3.41–3.55 [m, 4H, (N–CH_2–CH_2–$(CH_2)_{15}$–CH_3) × 2], 4.22–4.41 [bs, 2H, –NH_2–C_6H_5], 6.43 [d, 1H, $J = 5.2$ Hz, H-5-benzothiazole], 6.67 [s, 1H, H-7-benzothiazole], 6.99 [d, 1H, $J = 5.2$ Hz, H-4-benzothiazole]. ESI-MS m/z: 685 $[M]^+$.

4.3. Plasmids

*p*CMV-SPORT-β-gal was amplified in DH5α strain of *Escherichia coli*, isolated by alkaline lysis procedure and finally purified by PEG-

8000 precipitation as described previously [42]. The purity of plasmid was checked by A_{260}/A_{280} ratio (around 1.9) and 1% agarose gel electrophoresis.

4.4. Cells and cell culture

B16F10 (Human melanoma cancer cells), CHO (Chinese hamster ovary), A-549 (Human lung carcinoma cells) and MCF-7 (Human breast carcinoma cells) cell lines were procured from the National Centre for Cell Sciences (NCCS), Pune, India. Cells were cultured at 37 °C in Dulbecco's modified Eagle's medium (DMEM) with 10% Fetal Bovine serum, 50 μg/mL penicillin, 50 μg/mL streptomycin and 20 μg/mL kanamycin in a humidified atmosphere containing 5% CO_2.

4.5. Preparation of liposomes of lipids **1**–**10**

The cationic lipid and cholesterol in 1:1 mol ratio were dissolved in chloroform in a glass vial. The solvent was removed with a thin flow of moisture free nitrogen gas and the dried lipid film was then kept under high vacuum for 6 h. 1 mL of sterile deionized water was added to the vacuum dried lipid film and the mixture was allowed to swell overnight. The vial was then vortexed for 2–3 min at room temperature and then sonicated in bath sonicator followed by probe sonication in an ice bath until clarity using a Branson 450 sonifier at 100% duty cycle and 25 W output power to produce liposomes of lipids **1**–**10**.

4.6. Transfection biology

Cells were seeded at a density of 10,000 (for B16F10) and 15,000 cells (for CHO, A-549 & MCF-7) per well in a 96-well plate 18–24 h before the transfection. 0.3 μg (0.91 nmol) of plasmid DNA was complexed with varying amounts of lipids in plain DMEM medium (total volume made upto 100 μL) for 30 min. The charge ratios were varied from 1:1 to 8:1 over these ranges of the lipids. Just prior to transfection, cells plated in the 96-well plate were washed with PBS (2 × 100 μL) followed by the addition of lipoplexes. After 4 h of incubation, 100 μL of DMEM with 20% FBS was added to the cells. The medium was changed to 10% complete medium after 24 h and the reporter gene activity was estimated after 48 h. The cells were washed twice with PBS (100 μL each) and lysed in 50 μL Lysis buffer [0.25 M Tris–HCl (pH 8.0) and 0.5% NP40]. Care was taken to ensure complete lysis. The β-galactosidase activity per well was estimated by adding 50 μL of 2×-substrate solution [1.33 mg/mL of ONPG, 0.2 M sodium phosphate (pH 7.3) and 2 mM magnesium chloride] to the lysate in a 96-well plate. Absorbance of the product ortho-nitrophenol at 405 nm was converted to β-galactosidase units by using a calibration curve constructed using pure commercial β-galactosidase enzyme. Each transfection experiment was repeated three times on three different days. The transfection values reported were average values from three replicate transfection plates assayed on three different days. The values of β-galactosidase units in replicate plates assayed on the same day varied by less than 20%. The day to day variation in transfection efficiency values for identically treated transfection plates was mostly within 2–3 folds and was dependent on the cell density and condition of the cells.

4.7. Transfection biology in presence of serum

Cells were seeded at a density of 10,000 (for B16F10) and 15,000 cells (for CHO, A-549 & MCF-7) per well in a 96-well plate 18–24 h before the transfection. 0.3 μg (0.91 nmol) of plasmid DNA was complexed with lipids (**5**, **6**, **9** and **10**) in DMEM medium in presence of increasing concentrations of added serum (10–50%, v/v, and total volume made upto 100 μL) for 30 min. The lipid:DNA charge ratio of these lipoplexes were maintained as 8:1, at which all the lipids showed their highest transfection ability in all four types of cells used for transfection, (CHO, A-549, B16F10 and MCF-7). The remaining experimental procedure and determination of β-galactosidase activity per well is similar to that reported for the in vitro transfection experiments.

4.8. Cellular α5GFP expression study

For Cellular α5GFP expression experiments in CHO, 30,000 cells were seeded in each well of 24-well plate 18–24 h before the transfection. 0.9 μg of α5GFP plasmid DNA encoding green fluorescent protein was complexed with liposomes of lipids **1**–**10** at molar ratio (lipid:DNA) 8:1 in plain DMEM medium (total volume made upto 100 μL) for 30 min. Just prior to transfection, cells plated in the 24-well plate were washed with PBS (2 × 100 μL) followed by addition of lipoplexes. After 4 h of incubation 400 μL of complete media was added to the cells. After 24 h, the media was removed from each well and cells were washed with PBS (2 × 200 μL) and finally 200 μL of PBS was added to the cells and visualized under the inverted fluorescent microscope to observe the cells expressing the green fluorescent protein.

4.9. Cellular uptake observed under inverted microscope

Cells were seeded at a density of 10,000 cells/well in a 24 well plate usually 18–24 h prior to the treatment. *p*CMV-SPORT-β-gal DNA (0.3 μg of DNA diluted to 50 μL with serum free DMEM media) was complexed with rhodamine-PE labeled cationic liposomes (diluted to 50 μL with DMEM) using 8:1 lipid to DNA charge ratio. The cells were washed with PBS (1 × 200 μL), then treated with lipoplexes of lipids **1**–**10**, and incubated at a humidified atmosphere containing 5% CO_2 at 37 °C. After 4 h of incubation, the cells were washed with PBS (3 × 200 μL) to remove the dye completely from the wells and the cells were observed under inverted microscope.

4.10. Toxicity assay

Cytotoxicity of lipids **1**–**10** were assessed by the 3-(4,5-dimethylthiazol-2-yl)-2,5-diphenyltetrazolium bromide (MTT) reduction assay as described earlier [43]. The cytotoxicity assay was performed in 96-well plates by maintaining the same ratio of number of cells to amount of cationic lipid, as used in the transfection experiments. MTT was added 24 h after the addition of cationic lipids to the cells followed by 3 h of incubation. Results were expressed as percentage viability = [A_{540} (treated cells) − background/A_{540} (untreated cells) − background] × 100.

4.11. DNA binding assay

The DNA binding ability of the lipids **1**–**10** was assessed by conventional gel retardation assay on a 1% agarose gel (pre-stained with ethidium bromide) across the varying lipid:DNA charger ratios of 1:1 to 8:1. *p*CMV-β-gal (0.30 μg) was complexed with the varying amounts of cationic lipids in a total volume of 20 μL in DMEM and incubated at room temperature for 20–25 min. 4 μL of 6× loading buffer (0.25% Bromophenol blue in 40% (w/v)) sucrose in H_2O was added to it and the resulting solution (24 μL) was loaded on each well. The samples were electrophoresed at 80 V for 45 min and the DNA bands were visualized in the gel documentation unit.

4.12. DNase I sensitivity assay

Briefly, in a typical assay, 1.5 nmol of DNA (500 ng) was complexed with lipid using the indicated lipid:DNA charge ratios in

DMEM in a volume of 40 μL and the mixture was incubated at room temperature for 30 min on a rotary shaker. Subsequently, the complexes were treated with DNase I (at a final concentration of 1 ng/1.5 nmol of DNA) in presence of 10 mM $MgCl_2$ and incubated for 20 min at 37 °C. The reactions were then halted by adding EDTA (to a final concentration of 50 mM) and incubated at 60 °C for 10 min in water bath. The aqueous layer was washed with 50 μL of phenol: chloroform mixture (1:1, v/v) and centrifuged at 10,000 *g* for 5 min. The aqueous supernatants were separated, loaded (15 μL) on a 1% agarose gel, and electrophoresed at 100 V for 1 h. The bands were visualized with ethidium bromide staining.

4.13. Zeta potential (ξ) and size measurements

The sizes and the surface charges (zeta potentials) of liposomes and lipoplexes were measured by photon correlation spectroscopy and electrophoretic mobility on a Zetasizer $3000HS_A$ (Malvern, U.K.). The sizes were measured in Dulbecco's modified Eagle's medium (DMEM) with a sample refractive index of 1.59 and a viscosity of 0.89. The system was calibrated by using the 200 nm ± 5 nm polystyrene polymer (Duke Scientific Corps., Palo Alto, CA). The diameters of liposomes and lipoplexes were calculated by using the automatic mode. The zeta potential was measured using the following parameters: viscosity, 0.89 cP; dielectric constant, 79; temperature, 25 °C; *F*(*Ka*), 1.50 (Smoluchowski); maximum voltage of the current, V. The system was calibrated by using DTS0050 standard from Malvern. Measurements were done 10 times with the zero-field correction. The potentials were calculated by using the Smoluchowski approximation.

4.14. Statistical analysis

Data were expressed as mean ± standard error. Statistical analyses were performed using Student's *t* test for comparison of means. A probability of less than 0.005 was considered to be statistically significant.

Acknowledgment

Financial supports for this work from Department of Science and Technology, DST (to P.V. Srilakshmi.), Government of India, New Delhi and from National Institute of Technology, Warangal (the doctoral research fellowship to K. Bhavani) are gratefully acknowledged. We greatly acknowledge Dr. Arabinda Chaudhuri and Dr. Rajkumar Banerjee of Division of Lipid Science and Technology, Indian Institute of Chemical Technology, Hyderabad, India and their group for extending the tissue culture lab facilities to us and also for their immense help in carrying out the transfection experiments.

Appendix A. Supplementary data

Supplementary data related to this article can be found at http://dx.doi.org/10.1016/j.ejmech.2013.08.034.

References

[1] P.L. Felgner, T.R. Gadek, M. Holm, R. Roman, H.W. Chan, M. Wenz, J.P. Northrop, G.M. Ringold, M. Danielsen, Proc. Natl. Acad. Sci. U. S. A. 84 (1987) 7413–7417.
[2] P.L. Felgner, G.M. Ringold, Nature 337 (1989) 387–388.
[3] J.P. Behr, Tetrahedron Lett. 27 (1986) 5861–5864.
[4] J.P. Behr, B. Demeneix, J.P. Loeffler, J. Perez-Mutul, Proc. Natl. Acad. Sci. U. S. A. 86 (1989) 6982–6986.
[5] P. Pinnaduwage, L. Schmitt, L. Huang, Biochim. Biophys. Acta 985 (1989) 33–37.
[6] X. Gao, L. Huang, Biochem. Biophys. Res. Commun. 179 (1991) 280–285.
[7] G. Byk, D. Scherman, Expert Opin. Ther. Pat. 8 (9) (1998) 1125–1141.
[8] D. Scherman, M. Bessodes, B. Cameron, J. Herscovici, B. Hofland, F. Pitard, P.W. Soubrier, J. Crouzet, Curr. Opin. Biotechnol. 9 (5) (1998) 480–485.
[9] J. Zabner, Adv. Drug Deliv. Rev. 27 (1997) 17–28.
[10] A.D. Miller, Angew. Chem. Int. Ed. Engl. 37 (13–14) (1998) 1768–1785.
[11] K. Bhavani, P.V. Srilakshmi, Mol. Pharm. 9 (5) (2012) 1146–1162.
[12] M. Srujan, V. Chandrashekhar, R.C. Reddy, R. Prabhakar, B. Sreedhar, A. Chaudhuri, Biomaterials 32 (22) (2011) 5231–5240.
[13] K. Bhavani, P.V. Srilakshmi, J. Med. Chem. 54 (2) (2011) 548–561.
[14] K. Bhavani, P.V. Srilakshmi, Bioconjug. Chem. 22 (12) (2011) 2581–2592.
[15] M. Nishikawa, L. Huang, Hum. Gene Ther. 12 (2001) 861–870.
[16] M.T. Da Cruz, S. Simoes, P.P. Pires, S. Nir, M.C. de Lima, Biochim. Biophys. Acta 1510 (2001) 136–151.
[17] M.A. Iliesa, B.H. Johnsonb, F. Makorib, A. Millerb, W.A. Seitza, Arch. Biochem. Biophys. 435 (2005) 217–226.
[18] A. Roosjen, J. Smisterova, C. Driessen, J.T. Anders, A. Wagenaar, Eur. J. Org. Chem. (2002) 1271–1277.
[19] M.A. Ilies, W.A. Seitz, I. Ghiviriga, B.H. Johnson, A. Miller, J. Med. Chem. 47 (2004) 3744–3754.
[20] I. Solodin, C. Brown, M.S. Bruno, C.Y. Chow, E.H. Jang, Biochemistry 34 (1995) 13537–13544.
[21] M.A. Masloy, N.G. Morozoya, G.A. Serebrennikova, Mendeleev Commun. 10 (2000) 65–66.
[22] T.V. Konstantinova, V.N. Klykov, G.A. Serebrennikova, Russ. J. Bioorg. Chem. 27 (2001) 477–481.
[23] B. Avinash, P. Bishwajit, S.S. Indi, K. Paturu, B. Santanu, Bioconjug. Chem. 18 (6) (2007) 2144–2158.
[24] I.M. Baltork, A.R. Khosropour, S.F. Hojati, Monatsh. Chem./Chem. Monthly 138 (2007) 663–667.
[25] S.N. Manjula, N.M. Noolvi, K.V. Parihar, S.A. Reddy, V. Ramani, A.K. Gadad, G. Singh, N.G. Kutty, M. Rao, Eur. J. Med. Chem. 44 (2009) 2923–2929.
[26] B. Ballou, L.A. Ernst, A.S. Waggoner, Curr. Med. Chem. 12 (2005) 795–805.
[27] K. Licha, Top. Curr. Chem. 222 (2002) 1–29.
[28] J.V. Frangioni, Curr. Opin. Chem. 7 (2003) 626–634.
[29] D.D. Lasic, CRC Press, Boca Raton, 1997.
[30] C.J. Wheeler, L. Sukhu, G. Yang, Y. Tsai, C. Bustamente, Biochim. Biophys. Acta 1280 (1996) 1–11.
[31] M.E. Ferrari, D. Rusalov, J. Enas, C.J. Wheeler, Nucleic Acid. Res. 29 (2001) 1539–1548.
[32] K. Mukherjee, J. Bhattacharyya, J. Sen, R. Sistla, A. Chaudhuri, J. Med. Chem. 51 (2008) 1967–1971.
[33] R. Mukthavaram, S. Marepally, M.Y. Venkata, G.N. Vegi, R. Sistla, A. Chaudhuri, Biomaterials 30 (12) (2009) 2369–2384.
[34] K. Crook, B.J. Stevenson, M. Dubouchet, D.J. Porteous, Gene Ther. 5 (1998) 137–143.
[35] S. Li, M.A. Rizzo, S. Bhattacharya, L. Huang, Gene Ther. 5 (1998) 930–937.
[36] J. Turek, C. Dubertret, G. Jaslin, K. Antonakis, D. Scherman, B. Pitard, J. Gene Med. 2 (2000) 32–40.
[37] J.G. Lewis, K.Y. Lin, A. Kothavale, W.M. Flanagan, M.D. Matteucci, R.B. DePrince, R.A. Mook Jr., R.W. Hendren, R.W. Wagner, Proc. Natl. Acad. Sci. U. S. A. 93 (1996) 3176–3181.
[38] T. Joseph, D. Catherine, J. Gabrielle, A. Kostas, S. Daniel, P. Bruno, J. Gene Med. 20 (2000) 32–40.
[39] E. Virginie, C. Carole, L. Florence, B. Gerardo, S. Daniel, W. Pierre, Biochim. Biophys. Acta 1368 (1998) 276–288.
[40] M.T. Kennedy, E.V. Pozharski, V.A. Rakhmanova, R.C. MacDonald, Biophys. J. 78 (3) (2000) 1620–1633.
[41] M. Baichao, Z. Shubiao, J. Huiming, Z. Budiao, L. Hongtao, J. Control. Release 123 (2007) 184–194.
[42] J. Sambrook, E.F. Fritsch, T. Maniatis, Molecular Cloning a Laboratory Manual, second ed., Cold Spring Harbor Laboratory. Press, Cold Spring Harbor, NY, 1989.
[43] M.-B. Hansen, S.E. Neilson, K. Berg, J. Immunol. Methods 119 (1989) 203–210.